Estimation of TSS and Chl-a Concentration from Landsat 8-OLI: The Effect of Atmosphere and Retrieval Algorithm

Lalu Muhamad Jaelani[1], Resti Limehuwey[1], Nia Kurniadin[1], Adjie Pamungkas[2],
Eddy Setyo Koenhardono[3], and Aries Sulisetyono[4]

Abstract—**TSS and Chl-a are globally known as a key parameter for regular seawater monitoring. Considering the high temporal and spatial variations of water constituent, the remote sensing technique is an efficient and accurate method for extracting water physical parameters. The accuracy of estimated data derived from remote sensing depends on an accurate atmospheric correction algorithm and physical parameter retrieval algorithms. In this research, the accuracy of the atmospherically corrected product of USGS as well as the developed algorithms for estimating TSS and Chl-a concentration using Landsat 8-OLI data were evaluated. The data used in this study was collected from Poteran's waters (9 stations) on April 22, 2015 and Gili Iyang's waters (6 stations) on October 15, 2015. The low correlation between *in situ* and Landsat $Rrs(\lambda)$ (R^2 = 0.106) indicated that atmospheric correction algorithm performed by USGS has a limitation. The TSS concentration retrieval algorithm produced an acceptable accuracy both over Poteran's waters (*RE* of 4.60% and R^2 of 0.628) and over Gili Iyang's waters (*RE* of 14.82% and R^2 of 0.345). Although the R^2 lower than 0.5, the relative error was more accurate than the minimum requirement of 30%. Whereas, the Chl-a concentration retrieval algorithm produced an acceptable result over Poteran's waters (*RE* of 13.87% and R^2 of 0.416) but failed over Gili Iyang's waters (*RE* of 99.14% and R^2 of 0.090). The low correlation between measured and estimated TSS or Chl-a concentrations were caused not only by the performance of developed TSS and Chl-a estimation retrieval algorithms but also the accuracy of atmospherically corrected reflectance of Landsat product.**

Keywords—**remote sensing; water quality; TSS; Chl-a.**

Abstrak—**TSS dan Chl-a secara global dikenal sebagai parameter utama dalam pemantauan kualitas air laut. Mengingat tingginya variasi temporal dan spasial dari konstituen perairan, teknik penginderaan jauh adalah metode yang efisien dan akurat untuk mengekstrak parameter fisik air tersebut. Akurasi dari parameter fisik yang diturunkan dari data penginderaan jauh tergantung pada algoritma koreksi atmosfer dan algoritma estimasi parameter fisik yang akurat. Dalam penelitian ini, akurasi dari produk USGS yang terkoreksi secara atmosfer serta algoritma yang dikembangkan untuk menghitung konsentrasi TSS dan Chl-a menggunakan Landsat 8-OLI data telah dikaji. Data yang digunakan dalam penelitian ini dikumpulkan dari Perairan Poteran (9 stasiun) pada tanggal 22 April 2015, dan Perairan Gili Iyang (6 stasiun) pada tanggal 15 Oktober 2015. Korelasi yang rendah antara data *in situ* dan Landsat $Rrs(\lambda)$ (R^2 = 0,106) menunjukkan algoritma koreksi atmosfer yang digunakan oleh USGS memiliki keterbatasan. Algoritma estimasi konsentrasi TSS menghasilkan akurasi yang dapat diterima di Perairan Poteran (*RE* sebesar 4,60% dan R^2 sebesar 0,628) dan di perairan Gili Iyang (*RE* sebesar 14,82% dan R^2 sebesar 0,345). Meskipun R^2 lebih rendah dari 0,5, kesalahan relatifnya lebih akurat dari persyaratan minimum sebesar 30%. Sementara itu, algoritma estimasi konsentrasi Chl-a menghasilkan akurasi yang dapat diterima untuk Perairan Poteran (*RE* sebesar 13,87% dan R^2 sebesar 0,416) akan tetapi gagal di Perairan Gili Iyang (*RE* sebesar 99,14% dan R^2 sebesar 0,090). Korelasi yang rendah antara konsentrasi TSS atau Chl-a estimasi dan ukuran disebabkan tidak hanya oleh akurasi algoritma estimasi TSS dan Chl-a, tetapi juga oleh akurasi dari reflektan terkoreksi atmosfer dari produk Landsat.**

Kata Kunci—*penginderaan jauh; kualitas air; TSS; Chl-a*

I. INTRODUCTION

Remote sensing data have been widely used for monitoring the ecological, biological, and physical state of the seawater. Many studies have demonstrated that remote sensing imagery can be used for monitoring of the Chlorophyll-a (Chl-a) and Total Suspended Solid (TSS) concentrations. The range of 400 to 850 nm is often chosen for research aimed at determining methods for estimation of water quality parameters within the water column from remote sensing data [1]. The estimation of water quality parameters such as the concentration of TSS and Chl-a from satellite images is strongly depend on the accuracy of atmospheric correction and water quality parameter retrievals algorithms [2]–[7]. Atmospheric correction is a necessary process for quantitative monitoring of water quality parameters from satellite data.

In Indonesia's water, there was very limited algorithm developed and validated based on the *in situ* data of physical parameter as well as its reflectance data [7], [8]. Hence, the existing algorithm that was designed in different water area was directly implemented without considering the dynamic changes and the specific characteristics of local water in Indonesia.

Consequently, the objectives of the present study were 1) to evaluate the performance of atmospheric corrected

---

[1]Lalu Muhamad Jaelani, Resti Limehuwey, and Nia Kurniadin, Department of Geomatics Engineering, Faculty of Civil Engineering and Planning, Institut Teknologi Sepuluh Nopember, Surabaya, 60111, Indonesia. E-mail: lmjaelani@geodesy.its.ac.id, resti14@mhs.geodesy.its.ac.id, nia.kurniadin14@mhs.geodesy.its.ac.id.
[2]Adjie Pamungkas, Department of Urban and Regional Planning, Faculty of Civil Engineering and Planning, Institut Teknologi Sepuluh Nopember, Surabaya, 60111, Indonesia. E-mail: adjie@urplan.its.ac.id.
[3]Eddy Setyo Koenhardono, Department of Marine Engineering, Faculty of Marine Technology, Institut Teknologi Sepuluh Nopember, Surabaya, 60111, Indonesia. E-mail: eddy-koen@its.ac.id.
[4]Aries Sulisetyono Department of Naval Architecture and Shipbuilding Engineering, Faculty of Marine Technology, Institut Teknologi Sepuluh Nopember, Surabaya, 60111, Indonesia. E-mail: sulisea@na.its.ac.id.

reflectance data processed by USGS, and 2) to develop more accurate TSS and Chl-a concentration retrieval algorithms for Landsat 8-OLI data at Poteran and Gili Iyang's waters of Indonesia using *in situ* reflectance, TSS and Chl-a concentrations.

II. METHOD

A. Study Area

The data were collected from two water locations surrounding small islands in Indonesia. The first island is Poteran (7°5'11.88"S; 113°59'43.77"E), which is located in the southeast part of Madura Island, East Java Province and has a surface area of 49.8 km^2. At the south of the island, local community utilizes sea for seaweed farming. The second one is Gili Iyang (6°59'7.07"S; 114°10'32.22"E) which is located in the northeast of Madura Island, East Java Province and has a surface area of 9.15 km^2. The concentration of oxygen in this island is very high with average of 21.4 %. These two islands were separated by 22 km of distance. The locations of study area as well as the distribution of sample stations were shown in Figure 1. The waters surrounding this island were suffering with high loads of nutrients that indicated by high concentration of Chl-a (higher than 100 mg/m^3).

B. In situ Data Collection

To assess the performance of atmospheric corrected reflectance of Landsat product, the *in situ* spectra data and water quality concentration (i.e. TSS and Chl-a) were collected from Poteran's waters on April 22, 2015, the same time with Landsat 8-OLI acquisition. The same field campaign was performed over Gili Iyang's waters on October 15, 2015, except for spectra measurement which could not be measured by reason of strong wind speed. The data collecting station, which located less than one Landsat 8-OLI pixel (i.e. 30 m) away from the coastal area and corresponding Landsat 8-OLI pixels were contaminated by clouds were excluded from the analyses. Accordingly, 9 data (2 data without spectra) were used for Poteran area and 6 for Gili Iyang area.

All reflectance measurements were performed three hours before until three hours after 9.30 AM local time over optically deep waters. The water-leaving radiance ($L_u(\lambda)$), the downward irradiance ($E_d(\lambda)$), and the downward radiance of skylight ($L_{sky}(\lambda)$) were measured at each site using a Field Spec Hand Held (or Pro VNIR) spectroradiometer (Analytical Spectral Devices, Boulder, CO) in the range of 325–1075 nm at 1-nm intervals. The above-water remote-sensing reflectance ($Rrs(\lambda)$) was calculated approximately using the following equation [9]:

$$R_{rs}(\lambda) = \left(\frac{L_u(\lambda)}{E_d(\lambda)} - \frac{rL_{sky}(\lambda)}{E_d(\lambda)}\right) \times Cal(\lambda) \qquad (1)$$

where $Cal(\lambda)$ is the spectral reflectance of the grey reference panel that has been accurately calibrated, and r represents a weighted surface reflectance for the correction of surface-reflected skylight and is determined as a function of wind speed [9].

Concurrently, water samples were collected at nine and six stations over Poteran and Gili Iyang waters, respectively. Water samples were kept in ice boxes and taken to the laboratory for furthermore analysis. The chlorophyll-a were determined spectrometrically using

spectrophotometer. The optical density of the extracted Chl-*a* was measured at four wavelengths (750, 663, 645, and 630 nm), and the concentration was calculated according to SCOR-UNESCO's equations [10]. The total suspended solids were determined gravimetrically. Samples were filtered through pre-combusted whatman gf/f filters at 500°c for 4 hours to remove dissolved organic matter in suspension, which was then dried at 105°c for 4 hours and weighted to obtain TSS. The *in situ* remote sensing reflectance and water quality parameter collected over Poteran and Gili Iyang waters were presented in Table 1 and Figure 2.

C. Landsat 8-OLI Data Collection

Landsat 8-OLI data at path/row of 117/65 were collected at concurrent field campaign time. These data collected on April 22, 2015 and October 15, 2015. Since the atmospheric correction algorithm to convert remote sensing reflectance from Top of Atmospheric (TOA, recorded by sensor) to Bottom of Atmosphere (BOA, surface reflectance) is difficult for Landsat data, the Surface Reflectance (SR) which processed by USGS was used directly. The surface reflectance data was atmospheric corrected data using internal algorithm (for Landsat 8) and based on 6S algorithm for prior Landsat 8 for 7 bands. The information of Landsat band (excluded the TIR band) was presented in Table 2. These data could be ordered and downloaded from ESPA's website (http://espa.cr.usgs.gov/). The downloaded SR data then calibrated by dividing all digital numbers by 10000 and converted to remote sensing reflectance, $R_{rs}(\lambda)$, by dividing surface reflectance by π.

D. Accuracy Assessment

Assessment the accuracy of atmospheric correction algorithm developed by USGS and water quality parameter (TSS and Chl-a) retrieval algorithms used root mean square error (*RMSE*), relative error (*RE*) and determination coefficient (R^2). These notations were defined as follow:

$$RMSE = \sqrt{\frac{\sum_{i=1}^{N}\left(x_{esti,i} - x_{meas,i}\right)^2}{N}} \qquad (2)$$

$$RE = \frac{1}{N}\sum_{i=1}^{N}\left|\frac{x_{esti,i} - x_{meas,i}}{x_{meas}}\right| 100\% \qquad (3)$$

$$R^2 = \frac{1}{N}\sum_{i=1}^{N}\left(x_{esti,i} - x_{meas,i}\right)^2 \qquad (4)$$

where $x_{meas,i}$ and $x_{esti,i}$ are the measured and estimated values, respectively, and N is the number of samples. The *RMSE* gives the absolute scattering of the retrieved remote sensing reflectance as well as water quality parameter concentration, the *RE* represents the uncertainty associated with satellite-derived distribution and R^2 the strong relationship between *in situ* measured $R_{rs}(\lambda)$ and estimated $R_{rs}(\lambda)$ from atmospherically corrected of Landsat 8-OLI as well as measured and estimated water quality parameter (TSS and Chl-a) concentrations.

III. RESULTS AND DISCUSSION

A. Validation of Landsat Remote Sensing Reflectance

To validate the atmospheric corrected reflectance of Landsat (SR), the average of 3-by-3 window of Landsat pixel was used to compare with *in situ*-measured $Rrs(\lambda)$ in order to avoid potential error in the geometric correction and dynamics of water bodies, as well as the

potential error in spatial variability [11]. The *in situ* $Rrs(\lambda)$ measured by spectroradiometer in 1 nm interval was resampled to fit Landsat bands with the center of 440, 480, 560, 655, and 865 nm for band 1 to 7, respectively. Figure 3 showed the remote sensing reflectance comparison.

The data in Figure 3 shows that the water-leaving remote sensing reflectance $Rrs(\lambda)$ derived from Landsat 8 under estimate the *in situ* measurement Rrs(λ) at all observation stations except at the observation station of 1, 7 and 9 where the data were overestimation. The low relationship between two set of data indicated by low determination coefficient (R^2=0.106). However, all data comparisons between *in situ* and Landsat derived remote sensing reflectance have the same pattern.

B. TSS Concentration Retrieval Algorithm

The total suspended sediment concentration retrieval algorithm developed using the regression algorithm between the *in situ* TSS concentrations and *in situ* measured remote sensing reflectance $Rrs(\lambda)$ based on single-band and two-band ratios reflectance combinations. *In situ* TSS concentration and *in situ* $Rrs(\lambda)$ were used as dependent and independent variable, respectively. From several combinations, the highest correlation between both variables indicated by the highest coefficient of determination (R^2) was chosen as a retrieval algorithm. The regression algorithm for TSS concentrations was shown in Tables 3 and 4. In these tables, high coefficient of determination ($R^2 > 0.5$) were shown in the algorithm based on the band ratio of $Rrs(\lambda_2)/Rrs(\lambda_3)$, $Rrs(\lambda_2)/Rrs(\lambda_4)$ and $Rrs(\lambda_1)/Rrs(\lambda_4)$.

$$\log(TSS) = 1.5212 \left(\frac{\log R_{rs}(\lambda_2)}{\log R_{rs}(\lambda_3)} \right) - 0.3698 \qquad (5)$$

The highest correlation produced by an algorithm based on $Rrs(\lambda_2)/Rrs(\lambda_3)$ with R^2 of 0.79. This band-ratio based algorithm was used to calculate estimation of TSS concentration. The linier regression algorithm for TSS estimation with independent variable of band-ratio of $Rrs(\lambda_2)/Rrs(\lambda_3)$ was shown in Figure 4 and Equation 5.

C. Chl-a Concentration Retrieval Algorithm

The Chlorophyll-a concentration retrieval algorithm was made using regression algorithms based on single band and two band-ratios of Landsat 8 following the TSS retrieval algorithm. The regression algorithm of Chl-a concentrations were presented in Tables 5 and 6, for single band and two band-ratio combinations, respectively. In these tables, a high determination coefficient ($R^2 > 0.5$) were shown in band-ratio of $Rrs(\lambda_1)/Rrs(\lambda_4)$, $Rrs(\lambda_2)/Rrs(\lambda_3)$, and $Rrs(\lambda_2)/Rrs(\lambda_4)$ with the highest correlation produced by $Rrs(\lambda_2)/Rrs(\lambda_4)$ with R^2 of 0.63. The linier regression algorithm for Chl-a estimation with independent variable of band-ratio of $Rrs(\lambda_2)/Rrs(\lambda_3)$ for Poteran's waters was shown in Figure 5 and Equation 6.

$$\log(Chl - a) = 1.613 \left(\frac{\log R_{rs}(\lambda_2)}{\log R_{rs}(\lambda_4)} \right) + 1.0718 \qquad (6)$$

The algorithm produced the highest correlation with coefficient determination of 0.626.

D. Estimation of TSS Concentration and Its Validation

To assess the performance of the developed algorithms, the accuracy between measured data and estimated TSS were tested using *RMSE* and *RE*. The comparisons between the *in situ*-measured and Landsat-derived TSS concentrations over Poteran and Gili Iyang's waters were presented in Figures 5 and 6. Over Poteran's waters, the regression algorithm for estimating TSS concentration produced the highest accuracy with R^2 of 0.628; *RE* of 4.60%; and *RMSE* of 1.124. Whereas, over Gili Iyang waters, the algorithm produced the highest accuracy with R^2 of 0.345; *RE* of 14.823%; and *RMSE* of 2.916.

E. Estimation of Chl-a Concentration and Its Validation

The accuracy assessment of estimated Chl-a concentration from Landsat data followed the same step as TSS assessment. The regression algorithm for estimating Chl-a concentration over Poteran's waters produced high accuracy with R^2 of 0.416; *RE* of 13.873%; and RMSE of 68.645. Whereas over Gili Iyang's waters, the R^2, *RE* and *RMSE* were 0.090; 99.140% and 129.690, respectively (Figures 8 and 9).

Spatial distribution of TSS and Chl-a concentrations were processed using the previous developed algorithms shown in Figure 10.

CONCLUSION

This study was performed over Poteran's waters (9 stations) and Gili Iyang's waters (6 stations). Over these area, the *in situ* remote sensing reflectance $R_{rs}(\lambda)$, Chl-a and TSS concentrations were collected as well as Landsat-8 OLI data on the same acquisition time with *in situ* data. Low correlation between *in situ* and Landsat $R_{rs}(\lambda)$ (R^2=0.106) indicated that atmospheric correction algorithm performed by USGS has a limitation. This phenomenon was also reported by Jaelani [12], using a set of high quality *in situ* reflectance data collected over Lake Kasumigaura, Japan.

The *in situ* data was used to develop an applicable physical parameter retrieval algorithm for Chl-a and TSS concentration. The accuracy of algorithms were assessed using *in situ* data collected at the same acquisition time of Landsat 8 satellite. The TSS concentration retrieval algorithm produced acceptable accuracy both over Poteran's waters (*RE* of 4.60% and R^2 of 0.628) and over Gili Iyang's waters (*RE* of 14.82% and R^2 of 0.345). Although the R^2 lower than 0.5, the *RE* was more accurate than the minimum requirement of 30%. Whereas, the Chl-a concentration retrieval algorithm produced acceptable result over Poteran (*RE* of 13.87% and R^2 of 0.416) and failed over Gili Iyang's waters (*RE* of 99.14% and R^2 of 0.090). This indicated that the condition of chlorophyll-a over two waters is different. The low correlation between TSS and Chl-a measured, also estimated TSS and Chl-a concentrations were caused not only by performance of the developed TSS and Chl-a estimation retrieval algorithms but also the accuracy of atmospheric corrected reflectances of Landsat product.

REFERENCES

[1] A. G. Dekker, "Detection of Optical Water Quality Parameters for Eutrophic Waters by High Resolution Remote Sensing," Vrije Universiteit, Amsterdam, 1993.

[2] K. G. Ruddick, F. Ovidio and M. Rijkeboer, "Atmospheric Correction of SeaWiFS Imagery for Turbid Coastal and Inland Waters," *Applied Optics,* vol. 39, no. 6, p. 897–912, 2000.

[3] S. Sathyendranath, L. Prieur and A. Morel, "An Evaluation of The Problems of Chlorophyll Retrieval from Ocean Colour, for Case 2 Waters," *Advances in Space Research,* vol. 7, no. 2, p. 27–30, 1987.

[4] W. Yang, B. Matsushita, J. Chen and T. Fukushima, "Estimating Constituent Concentrations in Case Ii Waters from MERIS Satellite Data by Semi-Analytical Model Optimizing and Look-Up Tables," *Remote Sensing of Environment,* vol. 115, no. 5, p. 1247–1259, 2011.

[5] L. M. Jaelani, B. Matsushita, W. Yang and T. Fukushima, "Evaluation of Four MERIS Atmospheric Correction Algorithms in Lake Kasumigaura, Japan," *International Journal of Remote Sensing,* vol. 34, no. 24, p. 8967–8985, 2013.

[6] L. M. Jaelani, B. Matsushita, W. Yang and T. Fukushima, "An Improved Atmospheric Correction Algorithm for Applying MERIS Data to Very Turbid Inland Waters," *International Journal of Applied Earth Observation and Geoinformation,* vol. 39, p. 128–141, 2015.

[7] N. Laili, F. Arafah, L. M. Jaelani, L. Subehi, A. Pamungkas, E. S. Koenhardono and A. Sulisetyono, "Development of Water Quality Parameter Retrieval Algorithms for Estimating Total Suspended Solids and chlorophyll-A Concentration using Landsat-8 Imagery," in *Joint International Geoinformation Conference ISPRS Ann. Photogramm. Remote Sens. Spatial Inf. Sci.*, Kuala Lumpur, Malaysia, 2015.

[8] L. M. Jaelani, F. Setiawan and H. Wibowo, "Pemetaan Distribusi Spasial Konsentrasi Klorofil-A dengan Landsat 8 di Danau Matano dan Danau Towuti , Sulawesi Selatan," in *Pertemuan Ilmiah Tahunan Masyarakat Ahli Penginderaan Jauh Indonesia XX,* Bogor, 2015.

[9] C. D. Mobley, "Estimation of The Remote-Sensing Reflectance from Above-Surface Measurements," *Applied Optics,* vol. 38, no. 36, pp. 7442-7455, 1999.

[10] SCOR-UNESCO, "Determination of Photosynthetic Pigment in Seawater, Monographs on Oceanographic Methodology," UNESCO, Paris, 1966.

[11] L. Han and K. J. Jordan, "Estimating and Mapping Chlorophyll-a Concentration in Pensacola Bay, Florida using Landsat ETM+ data," *International Journal of Remote Sensing,* vol. 26, no. 23, p. 5245–5254, 2005.

[12] L. M. Jaelani, F. Setiawan and B. Matsushita, "Uji Akurasi Produk Reflektan-Permukaan Landsat Menggunakan Data In situ di Danau Kasumigaura , Jepang," in *Pertemuan Ilmiah Tahunan Masyarakat Ahli Penginderaan Jauh Indonesia XX*, Bogor, 2015.
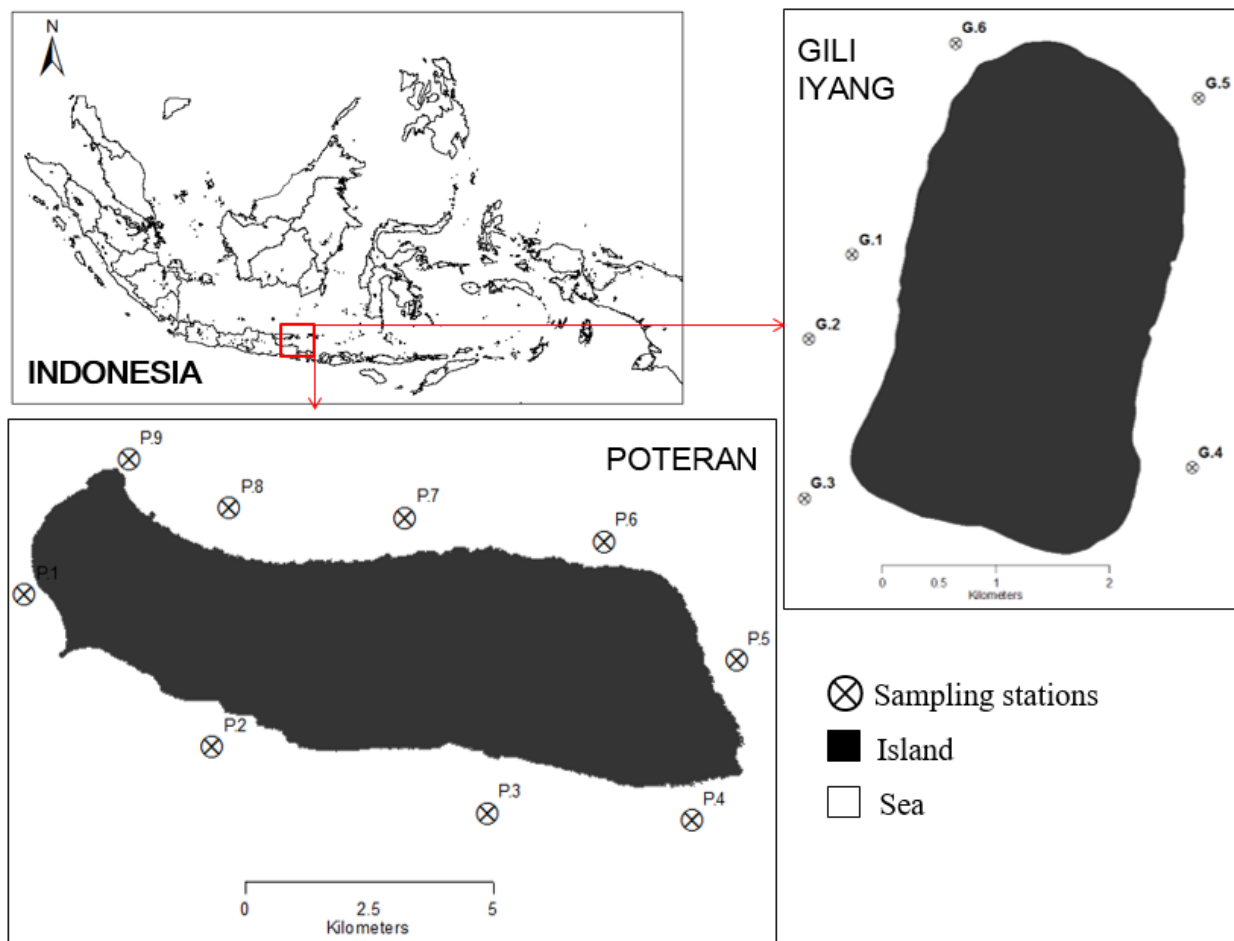
Figure. 1. The location and spatial distribution of the sampling station, "P "for Poteran and "G" for Gili Iyang waters
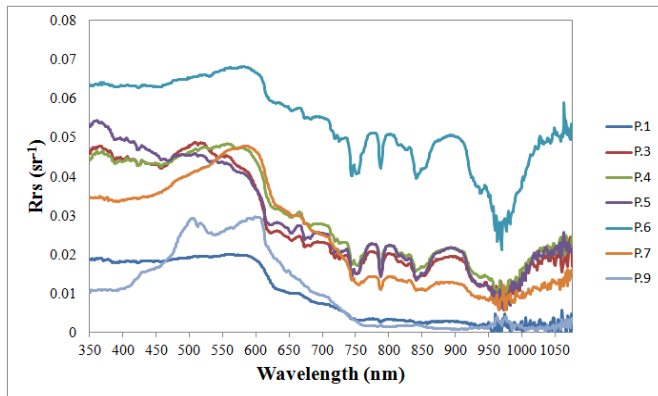
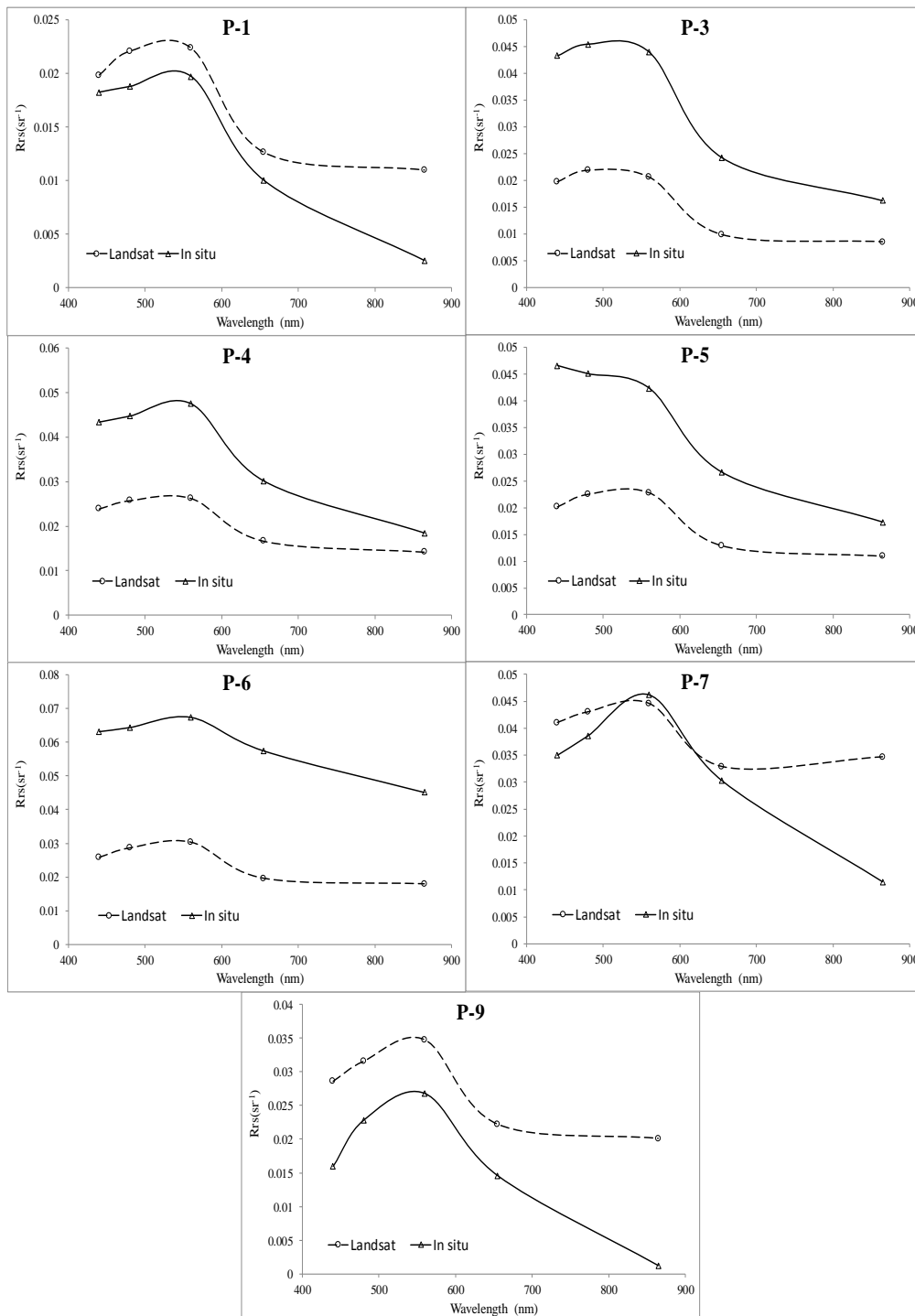Figure. 2. *In situ* spectral data collected over Poteran waters

Figure. 3. Comparisons between the *in situ*-measured and Landsat-derived water-leaving remote sensing reflectance
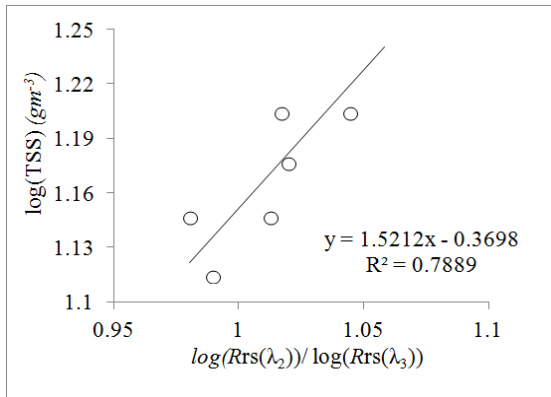
Figure. 4. Linier regression algorithm for TSS estimation with independent variable of band-ratio of $R_{rs}(\lambda_2)/R_{rs}(\lambda_3)$
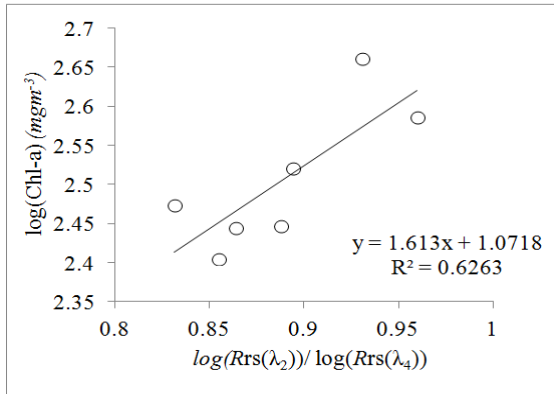

Figure. 7. Comparisons between the *in situ*-measured and Landsat-derived TSS concentrations over Gili Iyang's waters

Figure. 5. Linier regression algorithm for Chl-a estimation with independent variable of band-ratio of $Rrs(\lambda_2)/Rrs(\lambda_4)$

Figure. 8. Comparisons between the *in situ*-measured and Landsat-derived Chl-a concentrations over Poteran's waters
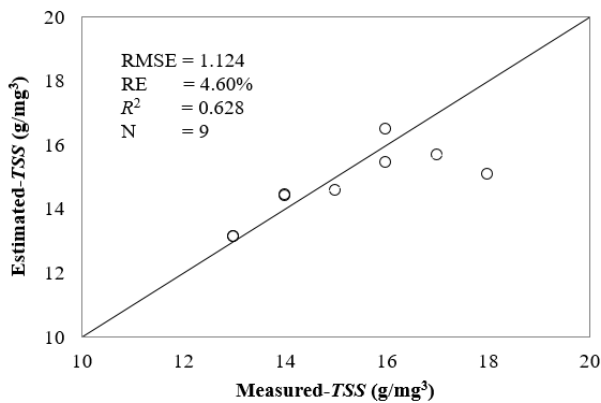

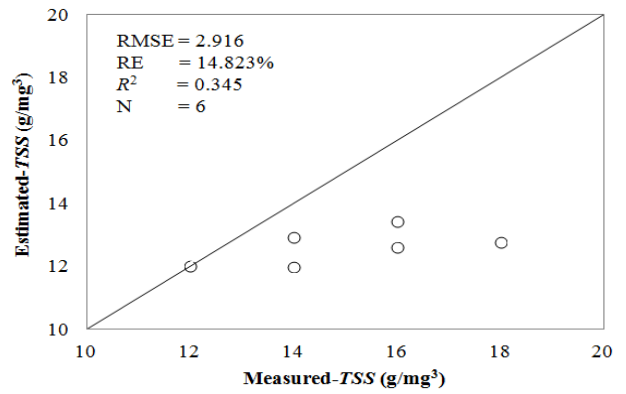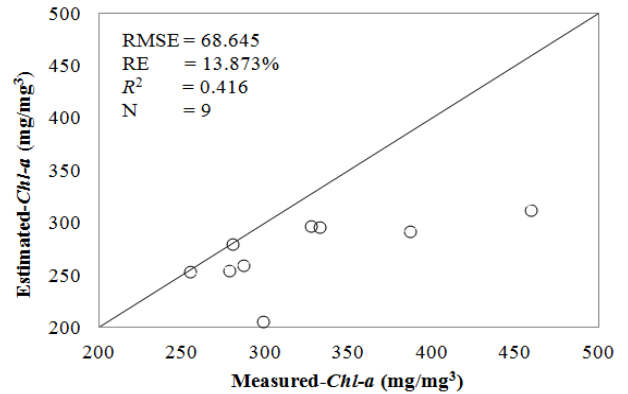
Figure. 6. Comparisons between the *in situ*-measured and Landsat-derived TSS concentrations over Poteran's waters
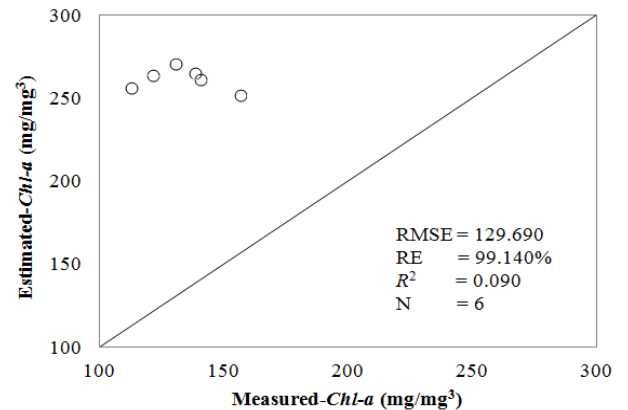

Figure.9. Comparisons between the *in situ*-measured and Landsat-derived Chl-a concentration over Gili Iyang's waters
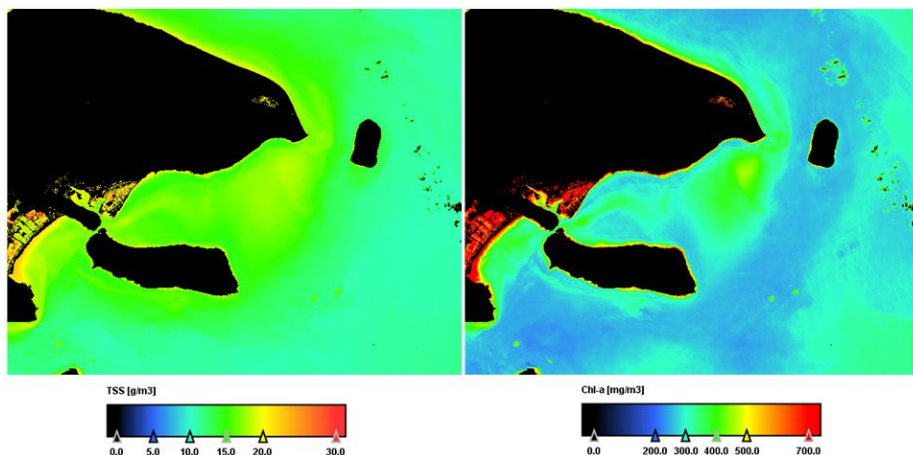

Figure.10. Distribution map of TSS (left) and Chl-a (right) concentration over Eastern Madura Sea

TABLE 1.
IN SITU SPECTRAL AND WATER QUALITY

Station	Location		Rrs (λ) (sr^{-1})					TSS	Chl	Depth
	Lat (°)	Long (°)	440 nm	480 nm	560 nm	655 nm	865 nm	(g/m^3)	(mg/m^3)	(m)
P-1	-7.0782	113.935	0.01823	0.01876	0.01971	0.01003	0.00255	14	278	3.8
P-2	-7.1058	113.969	0.0679	0.07301	0.06891	0.04308	0.04499	13	286	9
P-3	-7.1178	114.019	0.04327	0.04543	0.04396	0.02427	0.01624	13	298	10.1
P-4	-7.1191	114.056	0.0434	0.04474	0.04753	0.03017	0.01845	15	280	12.9
P-5	-7.0901	114.064	0.04661	0.04507	0.04237	0.02663	0.01729	14	254	8.5
P-6	-7.0686	114.04	0.06321	0.06442	0.06744	0.05746	0.0451	16	386	3.7
P-7	-7.0643	114.004	0.03498	0.03858	0.04618	0.03028	0.01151	18	459	4
P-8	-7.0624	113.972	0.10091	0.10964	0.11662	0.07857	0.07492	17	327	3.4
P-9	-7.0537	113.954	0.01594	0.02282	0.0268	0.01459	0.00122	16	332	13.9

TABLE 2.
LANDSAT 8-OLI BAND INFORMATION

Band	Wavelength (nm)			Central Wavelength	Bandwidth (nm)
1	430	-	450	440	20
2	450	-	510	480	60
3	530	-	590	560	60
4	640	-	670	655	30
5	850	-	880	865	30
6	1570	-	1650	1610	80
7	2110	-	2290	2200	180

TABLE 3.
SINGLE BAND-BASED REGRESSION ALGORITHM FOR TSS WITH R^2

Regresion Model	Band 1	Band 2	Band 3	Band 4	Band 5
$\log(TSS) = y_0 + a*b_j$	0.00	0.00	0.07	0.11	0.01
$\log(TSS) = y_0 + a*\log(b_j)$	0.00	0.00	0.06	0.10	0.00

TABLE 4.
TWO BAND RATIO-BASED REGRESSION ALGORITHM FOR TSS WITH R^2

Regresion Model	Band 1	Band 1	Band 1	Band 1	Band 2
	Band 2	Band 3	Band 4	Band 5	Band 3
$\log(TSS) = y_0 + a*(b_j/b_k)$	0.17	0.43	0.77	0.01	0.72
$\log(TSS) = y_0 + a*\log(b_j/b_k)$	0.15	0.39	0.77	0.00	0.72
$\log(TSS) = y_0 + a*(\log(b_j)/\log(b_k))$	0.17	0.47	0.77	0.01	**0.79**

Model Regresi	Band 2	Band 2	Band 3	Band 3	Band 4
	Band 4	Band 5	Band 4	Band 5	Band 5
$\log(TSS) = y_0 + a*(b_j/b_k)$	0.69	0.03	0.23	0.04	0.06
$\log(TSS) = y_0 + a*\log(b_j/b_k)$	0.65	0.01	0.22	0.02	0.08
$\log(TSS) = y_0 + a*(\log(b_j)/\log(b_k))$	0.73	0.00	0.24	0.04	0.14

TABLE 5.
SINGLE BAND-BASED REGRESSION ALGORITHM FOR CHL-A WITH R^2

Regresion Model	Band 1	Band 2	Band 3	Band 4	Band 5
$\log(chl\text{-}a) = y_0 + a*b_j$	0.01	0.05	0.17	0.21	0.06
$\log(chl\text{-}a) = y_0 + a*\log(b_j)$	0.01	0.04	0.14	0.18	0.02

TABLE 6.
TWO BAND RATIO-BASED REGRESSION ALGORITHM FOR CHL-A WITH R^2

Regresion Model	Band 1	Band 1	Band 1	Band 1	Band 2
	Band 2	Band 3	Band 4	Band 5	Band 3
log(chl-a)=y_0 + a*(b_j/b_k)	0.10	0.00	0.61	0.00	0.50
log(chl-a)=y_0 + a*log(b_j/b_k)	0.09	0.01	0.62	0.02	0.51
log(chl-a)=y_0 + a*(log(b_j)/log(b_k))	0.11	0.02	0.62	0.06	0.59

Model Regresi	Band 2	Band 2	Band 3	Band 3	Band 4
	Band 4	Band 5	Band 4	Band 5	Band 5
log(chl-a)=y_0 + a*(b_j/b_k)	0.57	0.00	0.24	0.00	0.01
log(chl-a)=y_0 + a*log(b_j/b_k)	0.59	0.01	0.24	0.00	0.01
log(chl-a)=y_0 + a*(log(b_j)/log(b_k))	**0.63**	0.02	0.24	0.00	0.04